MLI Blanket Effective Emittance Variance and its Effect on Spacecraft Propellant Line Thermal Control

Jennifer R. Miller[1], Pradeep Bhandari[2], Keith Novak[3], and Jacqueline Lyra[4]
Jet Propulsion Laboratory, California Institute of Technology, Pasadena, CA 91106

Multi-Layer Insulation (MLI) blankets commonly employed for temperature control of spacecraft propellant lines consistently show large variances in their effective emittances. These variances are primarily due to workmanship, hence are hard to control or predict. Unfortunately, the variances are also the primary drivers of propellant line temperatures, thus leading to large predicted temperature uncertainties and increased risks to the success of space missions.

JPL has gained significant knowledge of these variances from Mars spacecraft designs over more than two decades. This knowledge has led to improved analytical approaches to bound existing designs, emphasis on increased temperature visibility for design verification and model correlation, as well as methods for improving the robustness of propellant line thermal designs.

Nomenclature

AFT	=	Allowable Flight Temperature
JPL	=	Jet Propulsion Laboratory
MER	=	Mars Exploration Rovers
MLI	=	Multi-Layer Insulation
MPF	=	Mars Pathfinder
MSL	=	Mars Science Laboratory
PRT	=	Platinum Resistance Thermometer
SMAP	=	Soil Moisture Active Passive Mission
STV	=	Solar Thermal Vacuum

I. Introduction

Spacecraft liquid propulsion systems require thermal designs capable of maintaining hydrazine temperatures above a hard freezing limit (1.8°C) and below high temperatures that begin to degrade performance and/or affect secondary hardware. Filled prior to launch, propellant thermal control systems must maintain acceptable temperatures despite changing spacecraft environments and be ready to respond to requests for unplanned trajectory correction maneuvers such as those during fault responses. Propellant line thermal control is typically achieved by conductive isolation from the cold structure, a low emittance or multi-layer insulation (MLI) surface to reduce radiative exchange to the local surroundings, and heaters to provide localized heating. Propellant line temperatures are capable of changing quickly (on the order of 1°C/min) due to their low thermal capacitance and milliwatt heat balance (Fig. 1). Lateral line temperature gradients are created by factors such as low-conductivity metallic line materials (titanium, stainless steel), varying environmental sink temperatures depending on views to cold space or warmer spacecraft

[1] Engineer, Propulsion, Thermal & Materials Engineering Section, Jet Propulsion Laboratory, M/S 125-123, 4800 Oak Grove Drive, Pasadena, CA 91109.
[2] Principal Engineer, Propulsion, Thermal & Materials Engineering Section, Jet Propulsion Laboratory, M/S 125-123, 4800 Oak Grove Drive, Pasadena, CA 91109.
[3] Thermal Systems Engineer, Propulsion, Thermal & Materials Engineering Section, Jet Propulsion Laboratory, M/S 125-123, 4800 Oak Grove Drive, Pasadena, CA 91109.
[4] Project Delivery Manager, Propulsion, Thermal & Materials Engineering Section, Jet Propulsion Laboratory, M/S 125-123, 4800 Oak Grove Drive, Pasadena, CA 91109.

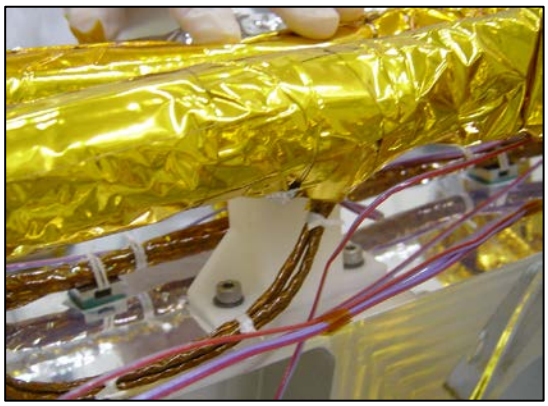

Figure 1: Example of Mount and Cable Heat Leaks

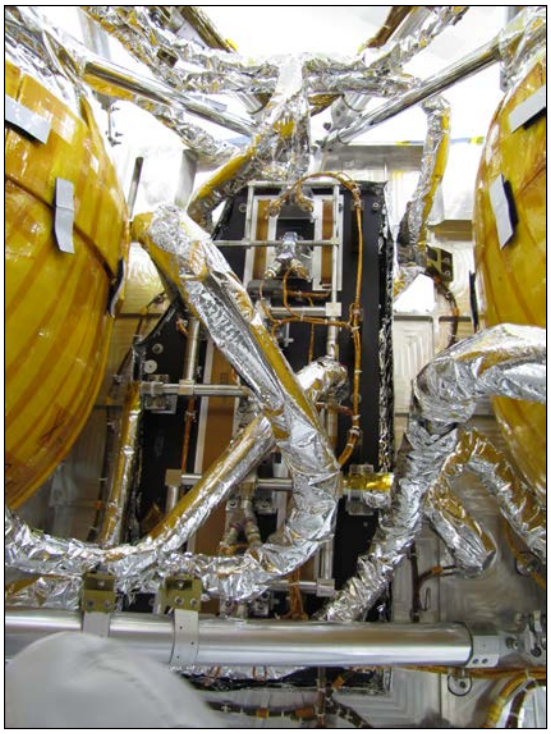

Figure 2: Non-Uniformity of MLI Propellant Line Installations

components, local conductive losses due to mechanical mounts and cable egresses, and finally due to Watt-density variations in line heaters.

The dependence of propellant line thermal design on MLI to provide radiative isolation creates an inherent vulnerability. MLI performance is extremely difficult to predict and repeat due to its non-uniformity when wrapped around small diameters involving bends, tees, egresses, close clearances, and access issues (Fig. 2). Performance is measured by an effective emittance (ε*), defined by (1):

$$\varepsilon^* = \frac{Q}{A\sigma(T_H^4 - T_C^4)} \tag{1}$$

where Q = heat transfer per unit time (W), σ = Stefan-Boltzmann constant (5.67E-8 W/m^2K^4), A = surface area (m^2), and T = temperature of the respective hot and cold surfaces and/or sinks (K).

MLI consists of multiple layers of low emittance materials to reduce heat transfer by radiation. Heritage JPL MLI designs use embossed materials or Dacron™/silk netting to reduce radial conduction through the blanket. Depending on location, additional layers such as beta cloth may be added to improve temperature capability or add micrometeoroid protection. Conduction dominates and MLI effectiveness decreases once these layers are compressed and conductive thermal shorts created. This happens at seams and when installation is impeded by factors such as those listed above. Conduction and radiation contributions (Ref. 2) are shown in (2).

$$q = \frac{C_S \bar{N}^{3.91} T_m}{N_S + 1}(T_H - T_C) + \frac{C_r \varepsilon_{RT}}{N_S}(T_H^{4.67} - T_C^{4.67}) \tag{2}$$

where q = heat flux per area (W/m^2), C_s = 4.43E-11, C_r = 8.03E-10, N = layers/cm, N_s = number of radiation shields, T = temperatures of the respective surfaces and sinks (K), $T_m = (T_H + T_C)/2$, and ε_{RT} = room temperature shield emittance.

Ideally, the conduction term in (2) would be zero, with all heat transfer occurring through radiation. For propellant lines with blankets only four to nine inches wide, a seam is always in close proximity and a significant fraction of the total area. Multiple blankets of ten to fifteen layers are used, installed with offset seams, to counteract the higher effective emittance at these locations. Installation, which so highly depends on workmanship, is difficult to do uniformly and repeatedly on anything other than a straight, accessible line.

II. MLI Considerations during Propellant Line Design

Propellant line thermal design is initially performed by assuming a "leaky" blanket, one with an effective emittance on the higher side of the credible range (0.05 to 0.30 per Ref. 1 however 0.10 is a more typical upper value based on JPL test history), to size heaters and ensure that temperatures can be maintained above freezing. Typically, higher values will be applied to bends to account for some reduction in performance due to MLI compression. Closed-loop thermal control, that autonomously modulates the heater duty cycle as needed, is established at the predicted coldest line location. The closed-loop heater control employed at JPL includes redundant flight temperature sensors connected to flight software, though earlier missions used mechanical thermostats (MPF). The long propellant line lengths are

divided into individually controlled discrete zones. Large propellant line zones may be constrained to a single control location due to limited resources such as flight temperature sensors or power switches in the flight electronics. The low lateral line conductance and varying parameters along the length (such as sink temperature, mounts and egress heat leaks, and MLI performance) combined with the single control point cause non-uniform temperature gradients with uniform heater duty cycles. Some of this variation can be accurately modeled and accounted for in a thermal model by varying heater density along the lines. However MLI variance is the most difficult parameter to predict and to bound.

In an effort to isolate the effect of MLI variance, a simplified calculation can be made ignoring all other factors except MLI variance. Table 1 shows the predicted temperature at location 2, given a control temperature of 25°C (constant heat flux applied by a single heater along the line length) at location 1. With a uniform MLI effective emittance, ε* (Case 1), temperatures remain uniform. In Case 2, with a good blanket at the control location 1 (low ε*) and a leaky blanket at another location 2 (high ε*), the second location freezes. However, reversing these ε* assumptions in Case 3 creates an overheating problem at location 2.

Table 1: Effect of MLI Variance. Temperature is controlled at location 1 and predicted at another location on the line, location 2.

Case	T_{sink}	control ε_1*	ε_2*	control T_1	T_2
1	-30°C	0.02	0.02	25°C	25°C
2	-30°C	0.02	0.10	25°C	-16°C
3	-30°C	0.10	0.02	25°C	127°C

Typically control points are located near standoffs with higher conductive loses and higher ε* values, causing overheating to be a higher risk. The conductive losses can be deterministically accounted for in the thermal model by estimating losses using known geometries and materials. Unfortunately test results have shown the chosen control location was not always the coldest location due to MLI variance and changes implemented during integration (such as cable routing).

Typical MLI ε* values for small propellant line blankets range from 0.05 to 0.30 (Ref. 1). Dedicated MLI thermal development tests conducted on various JPL flight programs attempted to better quantify these values and reduce performance uncertainty during the design phase. The only way to infer the as-built MLI ε* values is at the system-level test on the flight hardware. The introduction of judiciously placed non-flight test thermocouples provides additional comparison points from which to estimate the MLI ε* at many places along the line length in the analytical thermal model correlation to system test data. Although still providing only a discrete number of points, this allows for adjustments in heat loss along the length of the propellant lines. Since local conductive heat losses are automatically included in the correlation, MLI ε* adjustments can possibly mask other model inaccuracies if model-correlation knobs are turned blindly. In this way, it is not possible to state that correlated ε* values are exact or have tiny uncertainties, but this is the best method to create a final pre-launch thermal model for flight predictions. The only available line temperature telemetry available post launch is at the line control locations (known set temperatures) and perhaps a few additional flight sensors at nearby locations. The correlated thermal model affords the most insight into temperature gradients along the propellant lines of all zones.

III. Mars Mission Spacecraft Case Studies

JPL-led NASA Mars lander missions, over the past two decades, have presented an opportunity to gather data on propellant line performance and MLI variance for similar configurations. Mars Pathfinder (MPF), Mars Exploration Rovers (MER-A and MER-B), Mars Science Laboratory (MSL), and now Mars 2020 fly similar cruise stages scaled in size to meet the mission requirements (Table 2, Fig. 3). These spacecraft fly 6.35 mm stainless steel and titanium propellant lines mounted to a cruise stage structure with low conductivity brackets to carry hydrazine. A series of

Table 2: Comparison of Similar Mars Mission Propellant Systems

	MPF - Cruise Stage -	MER-A/MER-B - Cruise Stage -	MSL/Mars 2020 - Cruise Stage -	MSL/Mars 2020 - Descent Stage -
Length [m]	12	8	15	36
Line Diameter [mm]	6.35	6.35	6.35	6.35 to 25.4
Control Zones	4	8	15	21
Control Method	Mechanical Thermostat	Flight Software (Two Locations)	Flight Software (Single Location)	Flight Software (Single Location)
Correlated Model ε*	0.019 – 0.026	0.025 – 0.085	0.015 – 0.220	0.010 – 0.055

spiral heaters tuned for each location are installed on top of aluminum tape to increase lateral conduction and are then covered with MLI. The full line length is split into zones, each zone controlled by mechanical thermostats (MPF) or flight software located at the predicted coldest location. The design presents an additional challenge in that it is open bus, with the propellant system exposed to sink temperatures from -273°C to +100°C on the solar arrays. MSL and Mars 2020 also fly a second identical propulsion configuration on their descent stage, a system of 6.35 mm to 25.4 mm diameter lines encapsulated inside the aeroshell during the journey to Mars. This stage is dedicated to safely landing the rover on the Martian surface.

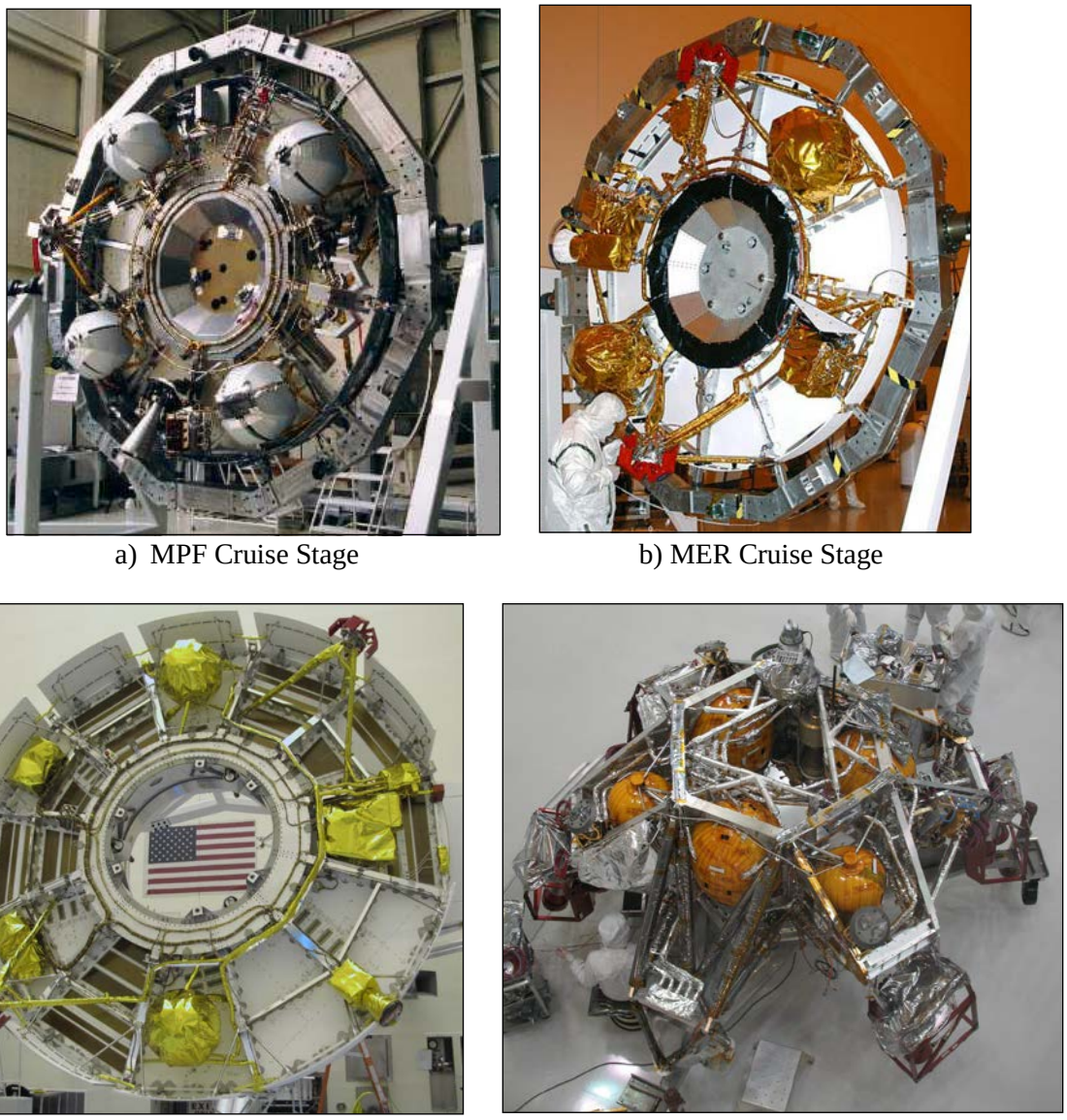

a) MPF Cruise Stage b) MER Cruise Stage

c) MSL Cruise Stage d) MSL Descent Stage

Figure 3: Mars Mission Spacecraft Stages with Propellant Systems

All JPL Mars missions above are thermal vacuum tested in the cruise configuration and separately tested in the landed configuration in a simulated Mars environment (typically 8 Torr GN_2). The cruise configuration stacks the rover and landing system (airbag protection or powered descent vehicle depending on the mission) inside the protective aeroshell attached to its respective cruise stage. Both the near-Earth hot and near-Mars cold cases are simulated in solar vacuum environments. Meanwhile, the landed configuration consists of a rover only. Since the propulsion system exists only on the cruise and landing elements, the stacked cruise configuration test becomes the most significant means for verification and validation of the propulsion thermal design. It also provides the opportunity to estimate the unknown MLI effective emittance.

With each of these correlations to Solar Thermal Vacuum (STV) test data, it is important to note that each thermal model, heater design, test, and correlation was performed by a different member of the JPL team over the past twenty-five years. Each thermal engineer had a slightly different approach and had progressively more detailed models as new tools become available. The MPF propellant line thermal model, initially created in SINDA-85 with ~500 nodes, has since evolved into the Mars 2020 cruise stage thermal model in Thermal Desktop with >20,000 nodes. Some engineers based their correlation of ε* off of the propellant line diameter, creating radiation couplings between line and external MLI nodes. More recently, the engineers have correlated ε* to the larger MLI diameter, modeling a separate MLI surface with the estimated ε* or a single surface with the MLI dimensions. The values shown in the following sections are estimates based on the larger external MLI area, depicting an effective emittance from the hardware outer surface (MLI) to the sink (shroud or nearby hardware). When needed, conversions were based on a geometry ratio of four (MLI diameter versus tube diameter) to allow a comparison between all Mars models.

A. Mars Pathfinder (MPF)

On MPF, the Cruise STV test identified both freezing and overheating concerns on the propellant lines. These concerns were enough to force a chamber break to implement possible fixes and require both a subsequent dedicated propellant line test and a new post-STV propulsion line thermal analysis. Another important STV discovery was that certain line sections, remotely located away from mechanical thermostat control points, would drop in temperature if the heaters were off for a long time; control locations had not been located at the coldest line location, as intended. Due to the use of mechanical thermostats, set points could not be updated from the initial 23°C/26°C (primary) and 18°C/21°C (secondary) design.

Test data from a dedicated propellant line test allowed model updates to the worst case ε* used in the thermal model. Initial estimates of 0.064 (global use) and 0.120 (local bends) for the original embossed Kapton MLI layup became 0.019 and 0.026 respectively for new Dacron net blankets. The decrease in effective emittance measured with the new blankets resulted in implementation on all the propellant lines even though these were only partially tested in the initial STV. In fact, the entire propulsion system was re-blanketed at Cape Kennedy prior to launch. The full flight implementation was not tested. This verification by analysis only, although not ideal, was thought to be the best path forward in order to protect the hardware and meet schedule. The following hardware changes were made to sections of the propellant lines during the chamber break and eventually implemented along all lines.

1. New 10-layer aluminized Mylar/Dacron net MLI installed (two offset blankets) with second surface aluminized Kapton overwrap replaced previous 15-layer embossed Kapton blankets. New blankets used a single seam along the length instead of seams at every edge.
2. Blankets added to line mounts to reduce heat loss.
3. Aluminum foil added along stainless steel lines to enhance lateral conduction.
4. 5-mil double-aluminized Mylar, semi-cylindrical radiation shields added to reduce mechanical thermostat views to warm solar array.

Lessons learned taken and improved upon by the next mission (MER) included: 1) the lack of set point adjustability offered by mechanical thermostats, 2) the need for more control zones, 3) the benefit of better representing view factors and sink temperatures (gradients over solar array for example), and 4) blanket workmanship identified as the greatest source of uncertainty.

B. Mars Exploration Rovers (MER)

A characterization test of MER MLI provided model inputs in order to understand the uncertainty without waiting for the system-level tests at later dates. The MLI layup of two 10-layer Kapton/Dacron net blankets was utilized as implemented on MPF. This test looked at blanketing straight, elbow and tee sections. The following results were found and implemented in the thermal model: ε* (straight) = 0.021 $\pm$ 0.005, ε* (elbow) = 0.046 $\pm$ 0.011, and ε* (tee) = 0.032 $\pm$ 0.009.

Despite identical designs and implementations, both the MER-A and MER-B spacecraft propellant lines performed differently in Cruise STV due to blanket installation workmanship. The thermal team avoided allowable flight temperature (AFT) violations and/or simultaneous A-side and B-side heater operation by updating set points during the tests for each zone – a capability that existed due to the change from mechanical thermostats (MPF) to flight-software controlled heaters (MER). MER-A and MER-B now each had unique set points at launch (Table 3). These

set points were further updated during flight using the correlated thermal model as solar flux decreased and prior to the turn-to-entry maneuver, a case inadvertently overlooked in early project phases that could have led to hydrazine freezing.

Table 3: Difference between MER-A and MER-B Propellant Line Set Points

	Design (Pre-Test)		MER-A (Post-Test)		MER-B (Post-Test)	
	On (°C)	Off (°C)	On (°C)	Off (°C)	On (°C)	Off (°C)
1A	30	40	30	37	28	34
2A	30	40	36	44	36	46
3A	30	40	36	44	37	43
4A	30	40	36	44	23	30
5A	30	40	36	44	34	43
6A	30	40	37	44	33	40
7A	30	40	31	40	31	40
8A	30	40	31	41	31	41
1B	27	33	38	44	31	41
2B	27	32	22	27	22	27
3B	27	32	24	30	24	30
4B	28	36	23	30	36	44
5B	28	36	23	31	23	31
6B	26	33	22	29	26	33
7B	25	35	26	35	26	35
8B	25	35	26	35	26	35

Beyond the difference in set points, an observation was made for Zones 1 and 4 on MER-B. A-side control locations were chosen as the predicted coldest point with B-side control locations at the second coldest elsewhere in the same zone. In these two zones, the B-side location was warm enough that when the zone was operated by the A-side heater, the B-side location could overheat. In order to prevent violating maximum AFTs, primary control was given to the B-side. It is often difficult to predict the correct sensor locations and too disruptive to the tested spacecraft and correlated model to uninstall tested MLI, change sensor locations, and reinstall un-tested MLI. A lesson learned and incorporated into the next mission (MSL) was to co-locate A and B sensors to avoid competing circuits.

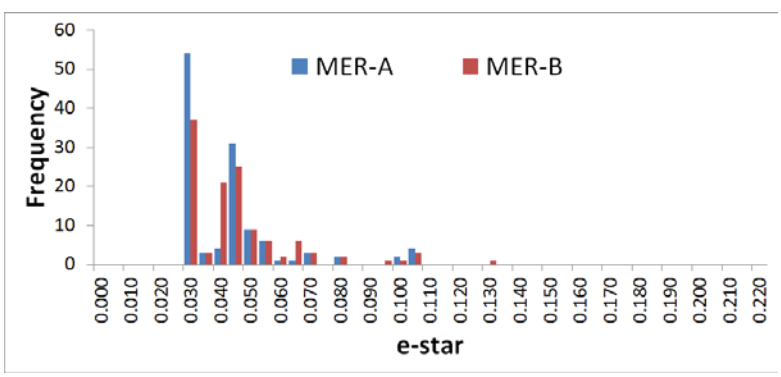

Figure 4: MER Correlated Thermal Model ε* Values

Model correlation updated set points to match those found in test and allowed an estimation of MLI ε* (Fig. 4). Although following a similar trend and aided by the ability to use the MER-A correlated model as a starting point for MER-B, values were not identical. Over both spacecraft, values were evident from 0.03 to 0.13, a ratio of 4:1, and higher than the maximum ε* value 0.046 ± 0.011 used in the original model by almost 50%.

C. Mars Science Laboratory (MSL)

In addition to the cruise stage, MSL included a descent stage to safely land the rover on the Martian surface. This added an additional 36 m of propulsion line routing, tightly packed, with varying diameters (from 6.35 mm to 25.4 mm). Mount conductance was calculated as low as 0.001 W/K for the longer mounts. During STV, much like MER, set points were adjusted by up to 11°C to avoid violating AFT limits. Original thermal model parameters used line MLI ε* values from a MSL propellant line development test (ε*(straight) = 0.032, ε* (bend) = 0.040, and ε* (fitting) = 0.050) as well as a conservative case of ε* = 0.082 globally. Although ensuring the heaters could handle a less optimal blanket, this uniform application of ε* did not highlight a worst case as described in Section II created by non-uniform blankets. Post-test correlation discovered outliers (ε* of 0.22), however the majority of values fell within an approximate 5:1 ratio (ε* of 0.01 to 0.10) shown in Fig. 5. As expected, bend and standoff locations consistently had higher correlated ε* values than the straight sections. The descent stage, with larger diameter lines, had lower ε* values than cruise stage.

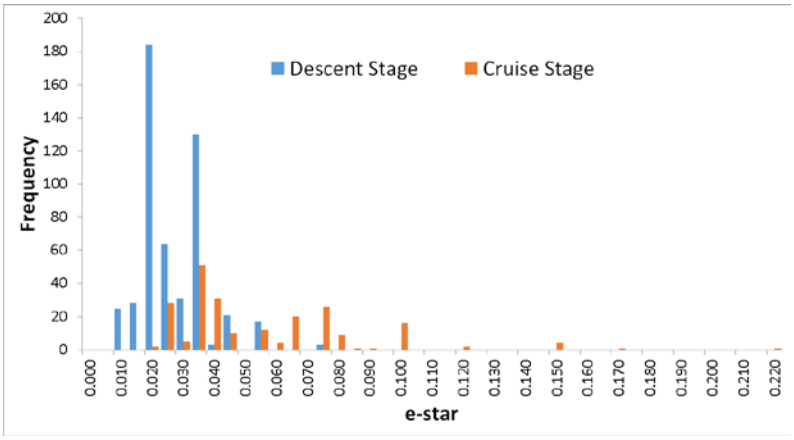

Figure 5: MSL Correlated Thermal Model ε* Values

D. Mars 2020

In an effort to incorporate MLI lessons learned in previous missions, Mars 2020 is incorporating the 5:1 $\varepsilon^*_{max}/\varepsilon^*_{min}$ ratio seen on MSL. This is an attempt to improve worst-case hot and cold predictions due to known MLI workmanship variations. This leads to a better system understanding and bounding of the credible worst-case extremes in the design phase, well ahead of the system thermal test. Mars 2020 propellant line set points can then be adjusted during test and later using an appropriately modified test-correlated model to better center temperatures.

While 5:1 is a large ratio, it is understood that ε* is often a value thermal engineers use to adjust heat balances and possibly account for missing heat leaks elsewhere (i.e. cable egresses, under-estimated line mount conductive or radiative losses). Model correlation to test data typically results in less than 5°C difference and this extends to temperatures found in flight. Although an ε* ratio of 5:1 is not an exact value, it appears to be properly representing the heat balance for a given design and thus a credible range for Mars 2020 as a build-to-print project from the MSL design.

IV. Current JPL Implementation

Recent JPL missions have improved propellant thermal design by enclosing the lines and avoiding the open bus design model. For example, the SMAP mission kept as much propellant line length as possible interior to its bus where a warmer environment could keep the lines within AFTs. On the exterior propellant lines, a MLI enclosure offset from the lines was created. Though it required more power to maintain temperatures, the system was no longer dependent on small heat balances and was thus more robust to variances in each zone.

However the threat of in-flight propellant line temperature violations continues to exist in the Mars 2020 open bus architecture, due to MLI workmanship variance, no matter what values are used to design the system. The goal is to be able to fix problem line temperatures using solutions that do not depend solely on MLI. Current best approaches for these problem areas are to adjust set points, and to make the system robust to begin with, so that any MLI combination can be successful. The thermal team has proposed an increase in aluminum tape from two to ten layers, to increase lateral conduction along the Mars 2020 propellant lines and reduce gradients. Although costly and time consuming, increasing aluminum tape layers over the line decreases the risk of finding a problem later during test and flight, but does not negate the risk. Complying with the project directive to minimize propellant line thermal design changes from successive missions requires subtle changes to improve robustness.

V. Conclusion

History has taught us that unavoidable workmanship variances in propellant line MLI performance will prompt changes in line set point temperatures and thermal model updates that can be achieved only through system thermal tests. Dedicated propellant line thermal tests provide insight into variations due to line routing but often do not translate well to the system model. The complicated nature of the spacecraft as a whole provides a more difficult heat balance to accurately model, and MLI effective emittance is often used as a knob to account for unknown heat leaks. To uncover the threat of in-flight propellant line temperature limit violations that would remain invisible due to sparse flight telemetry sensors, it is critical that the analytical thermal model be thoroughly exercised. It should employ not only an appropriate range of ε^* values, but avoid a global application of a single ε^* to understand how combinations of values affect the design space. Examples herein have shown MLI effective emittance to be off by as much as 50% and set point updates needed by up to 11°C.

The best approach is to create a thermal design less sensitive to inherent MLI variances. Robust design choices include: increased lateral conductance on the line using aluminum tape or foil, designs with a closed bus, larger heat balances, or more deterministic hardware emittances to name a few (Ref. 3). Propellant line control is a tough challenge that has plagued JPL thermal engineers for decades. JPL thermal engineers continue to increase knowledge and develop a better understanding of the nuances, but have yet to adopt a better design to avoid a dependence on MLI emittance. The goal here is to improve JPL analysis and test methods to better an existing design. A robust design and a correlated thermal model, with better MLI emittance estimations, will decrease the risk for any mission and provide the best tools to respond to in-flight anomalies.

Acknowledgments

The development described in this paper was carried out at the Jet Propulsion Laboratory, California Institute of Technology, under a contract with the National Aeronautics and Space Administration. The author would like to acknowledge the many thermal engineers who committed their time and energy to the above Mars missions. Much of the work detailed within was completed by the many who designed, implemented, tested, correlated, and successfully operated these missions. Copyright 2016 California Institute of Technology. Government sponsorship acknowledged.

References

1. Gilmore, David. *Spacecraft Thermal Control Handbook, Volume 1*. El Segundo, CA: The Aerospace Corporation, 2002.
2. Keller, C.W., Cunnington, G.R., and Glassford, A.P. *Thermal Performance of Multi-Layer Insulations, Final Report*. Sunnyvale, CA: Lockheed Missile and Space Company, 1974. Contract NAS3-14377.
3. Bhandari, P. *Robust Thermal Control of Propulsion Lines for Space Missions*. 46th International Conference on Environmental Systems (ICES), Vienna, Austria, July 10-14, 2016.
4. Novak, K. S., The Mars Pathfinder Propulsion Line Thermal Design: Testing, Analysis and Prelaunch Modifications." 9th Spacecraft Thermal Control Technology Workshop, El Segundo, CA. March 4-6, 1998.
5. Novak, K. S., Kinsella, G. M., Krylo, R. J., Sunada, E. T. *Thermal Design and Flight Experience of the Mars Exploration Rover Spacecraft Computer- Controlled, Propulsion Line Heaters*. 34th International Conference on Environmental Systems (ICES), Colorado Springs, Colorado, July 19-22, 2004.
6. Paris, A. D., et al. *Thermal Control of the Mars Science Laboratory Spacecraft Propellant Lines – Design Architecture and Analytical Modeling*. 41st International Conference on Environmental Systems (ICES), Portland, Oregon, July 17-21, 2011.
7. Bhandari, P. *Robust Thermal Control of Propulsion Lines for Space Missions*. 46th International Conference on Environmental Systems (ICES), Vienna, Austria, July 10-14, 2016.